Eur. Phys. J. D **26**, 105–109 (2003)
DOI: 10.1140/epjd/e2003-00085-9

THE EUROPEAN PHYSICAL JOURNAL D

Time-frequency characterization of high-order harmonic pulses

R. López-Martens[a], J. Mauritsson, A. Johansson, J. Norin, and A. L'Huillier

Department of Physics, Lund Institute of Technology, P.O. Box 118, 221 00 Lund, Sweden

Received 20 December 2002
Published online 24 April 2003 –

Abstract. We present energy-resolved cross-correlation measurements of extreme ultraviolet (XUV) pulses generated as high harmonics of femtosecond pulses from a 1 kHz titanium-sapphire laser. The harmonic pulses are probed by a fraction of the fundamental laser pulse at 800 nm, in a noncollinear geometry, allowing us to vary independently the parameters of the harmonic pump and near-infrared probe pulses. We measure the so-called "sidebands" in the photoelectron spectrum of argon corresponding to the absorption of a harmonic photon plus or minus one probe photon. Spectrally resolving the cross-correlation signal allows us to characterize the time-dependent frequency of the XUV pulse.

PACS. 42.65.Ky Harmonic generation, frequency conversion

1 Introduction

The characterization of high-order harmonics both in time and frequency is important for several reasons. The temporal phase of the harmonic field is directly related to the fundamental process behind harmonic generation. Indeed, the frequency modulation of the harmonic radiation originates in the extra phase that the electron wavepacket accumulates during its acceleration in the continuum, reflecting therefore the dynamics of the process [1,2]. In addition, macroscopic effects arising from phase matching and ionization can lead to frequency modulations [3–5]. Thus, the determination of the frequency variation of the harmonic radiation gives information both on the single-atom response and on phase-matching. Applications in time-resolved studies require full characterization of the temporal characteristics of the pump (harmonic) and probe pulses [6,7]. Finally, the understanding and control of high harmonic frequency modulations is crucial for the production of attosecond pulse trains [8] as well as of attosecond pulses [9]. If harmonics exhibit a significant order-dependent frequency variation (chirp), phase-locking is not possible, and no attosecond train can be generated [10].

Our method is based on the energy-resolved cross-correlation between the harmonics and a near-infrared (IR) laser pulse. When the two pulses overlap in time, sidebands appear in the photoelectron spectrum, corresponding to absorption of a harmonic photon together with absorption or emission of one or more IR photon. By delaying the two pulses with respect to each other, the duration of the harmonic pulse can be inferred from the time-dependent amplitude of the sidebands [11,12]. The location of the sideband in the photoelectron spectrum also depends on the delay between the pulses, and can be used to measure the time-dependent frequency of the harmonic. A chirped harmonic pulse gives rise to a tilted sideband when the photoelectron yield is plotted as a function of energy and time delay [5]. Alternative methods to determine the pulse duration and phase of the harmonics use the ponderomotive shift of the ionization potential (ponderomotive streaking) [13,14], or a two-photon ionization process [15].

This communication describes the progress made in Lund towards the full characterization in time of high-order harmonics. We summarize our first experimental results [5] obtained by using harmonics generated by 80 fs 400 nm radiation and probed with 50 fs 800 nm radiation. Then we describe more recent results where harmonics of order 19 to 25, generated by a 50 fs 820 nm laser, are probed by a 50 fs infrared laser. Finally, some preliminary results obtained with a sub-10 fs 820 nm probe will be briefly presented. After a description of our experimental method in Section 2, we present and discuss our results in Section 3, before concluding in Section 4.

2 Experimental setup

The different experimental configurations used closely resemble, in principle, the one described in [5]. We describe here briefly the setup, schematically depicted in Figure 1, employed to characterize harmonics generated by infrared 50 fs pulses, using a 50 fs infrared probe.

The harmonic radiation is generated by focusing a 1 mJ fraction of fundamental output from a 2 mJ 1 kHz 820 nm laser with a $f = 50$ cm lens through a 3 mm-long cell containing a 30 mbar static pressure of argon.

[a] e-mail: rodrigo.lopez@fysik.lth.se

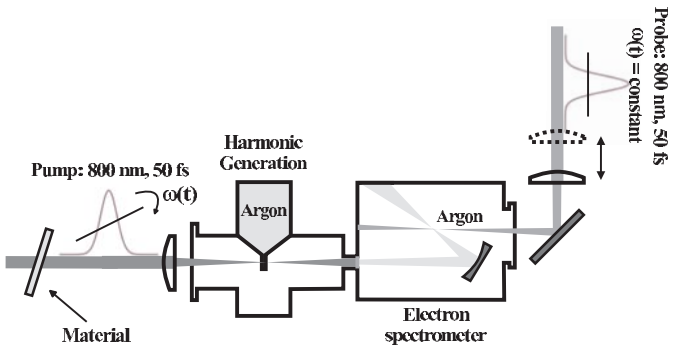

Fig. 1. Schematic description of the experimental setup.

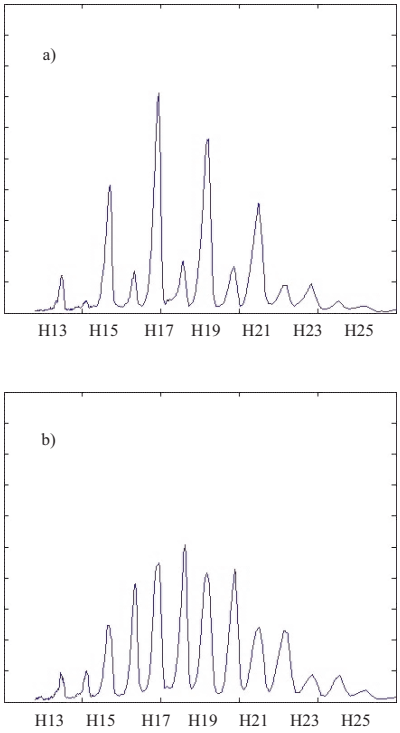

Fig. 2. Electron spectra; (a) with a weak probe, (b) with an intense probe.

The weakly diverging harmonic beam is passed through a 200 nm thick Al filter, to eliminate the residual infrared light, and focused approximately 1 m downstream by a +20 cm gold coated mirror into the sensitive region of a magnetic bottle spectrometer (MBES) filled with a background pressure argon of typically around 5×10^{-4} mbar.

In order to achieve day-to-day reproducibility, the gas cell was systematically placed close to the focus of the generating infrared beam and the latter was appropriately apertured so as to maximize the overall photoelectron yield due to ionization by the harmonics. The peak intensity of the laser was estimated to always lie close to saturation intensity for argon around 2×10^{14} W cm^{-2}.

Before the laser is sent in to generate the harmonics, a fraction of similar energy, constituting the probe, is picked off from the total laser output and re-routed through an independent delay stage and made to coincide in a non-collinear fashion with the harmonic beam inside the MBES. The focusing of the probe is performed using a +50 cm lens on a sliding mount which allows us to vary the size of the probe focus at its point of overlap with the harmonic beam. This is done not only to ensure that the harmonic beam experiences a constant probe intensity in the interaction region, but also to vary the intensity of the probe without affecting the delay between pump and probe.

A typical electron spectrum obtained with a weak probe is shown in Figure 2a. The regularly spaced most intense photoelectron peaks observed here correspond to ionization of argon by harmonics of the plateau ranging from orders 13 to 25. As harmonics in the plateau are generated with similar peak intensities, it is clear that the shape of the spectrum does not reflect true relative harmonic intensities but, instead, is mostly determined by the response function of the MBES itself. Adding a retarding voltage to the electron drift tube of the MBES allows us to observe the electronic signature of higher harmonic orders in the spectral cut-off. Up to harmonic 31 can be detected which corresponds quite well with the theoretical cut-off photon energy that can be expected for the generating laser intensity. The duration and phase of the infrared pump and probe pulses are controlled on a day to day basis using a SPIDER (Spectral Interferometry for Direct Electric field Reconstruction) [16]. The laser compressor is set so that the probe pulse is as short as possible (in accordance with the output laser spectrum) in the interaction region.

The weaker peaks in Figure 2a are the side-band signals, which can only be observed when spatial and temporal overlap between the pump and the probe pulses is realized. The advantage of our setup compared to previous ones [11–14] is that it is easy to manipulate both infrared beams independently. Figure 2b shows for example an electron spectrum obtained with a more intense probe, by moving the probe focusing lens (see Fig. 1). Sidebands as intense as the main harmonic peaks are observed. We have recently used our setup to study the influence of the angle between the polarization vectors of the probe and the pump on the sideband signals. We have also varied the ellipticity of the probe polarization from linear to circular [17].

3 Results and discussion

In our first demonstration of the method [5], we used frequency doubled light (of about 80 fs duration) to generate harmonics in xenon and 50 fs infrared probe pulses. The main advantage of this configuration was that the sidebands from two consecutive odd harmonics did not interfere, allowing us to characterize one harmonic at a time. A typical result obtained on the fifth harmonic is shown in Figure 3.

As shown by the tilted line going through the sideband signal, the energy of the photoelectron increases linearly as

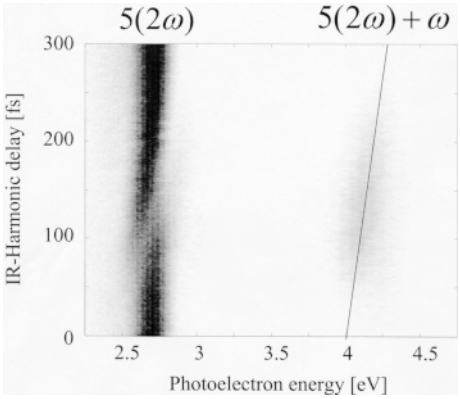

Fig. 3. Electron signal as a function of kinetic energy and time delay; the trace on the left is the "main" peak, corresponding to ionization of Xe gas at the 5th harmonic of the frequency doubled light, with the ion left in the $^2P_{3/2}$ core; the trace on the right is a sideband peak, obtained by absorption of the fifth harmonic plus an infrared photon, with the ion left in the $^2P_{3/2}$ core.

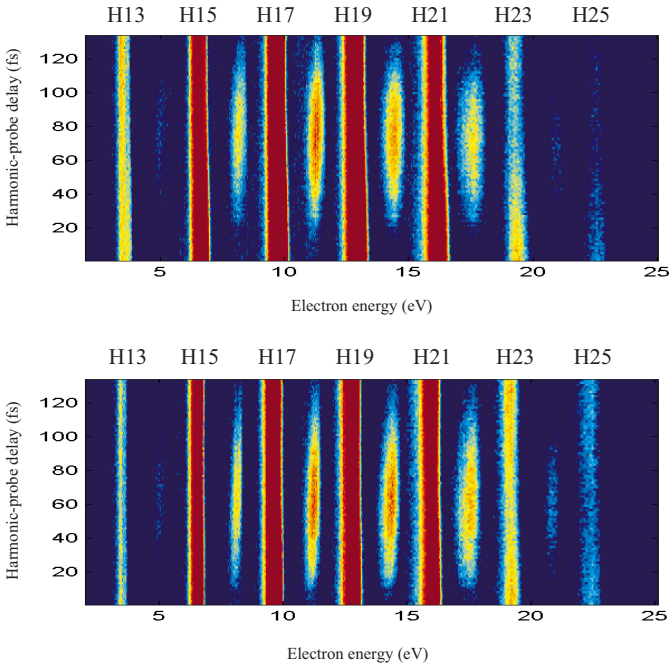

Fig. 4. Electron signal as a function of kinetic energy and time delay; (top) without and (bottom) with a 1 cm piece of BK7 glass in the path of the laser beam that generates the high-order harmonics.

the time delay increases. This shows evidence in this case for a linear positive chirp of the fifth harmonic. The right trace in Figure 3 clearly shows that the main peak, corresponding to absorption at the fifth harmonic frequency, is also strongly influenced by the presence of the probe beam. The photoelectron signal is slightly broadened, and depleted in an asymmetric way, reflecting the shape of the sideband trace. Three cases in which different amounts of chirp were imposed on the fundamental beam by going through glass plates were investigated. The probe beam was set to have zero chirp. The position of a sideband as a function of the probe delay was measured, and the slope in eV/fs was extracted. The sidebands are generated at the point of maximum temporal overlap between the pulses, and since the length of the probe pulse was of the same order of magnitude as that of the harmonics, the extracted harmonic chirp values had to be adjusted according to

$$\frac{b_{\text{true}}}{b_{\text{measured}}} = 1 + \left(\frac{\tau_{\text{probe}}}{\tau_{\text{harm}}}\right)^2 . \qquad (1)$$

Our results presented in more details in [5] show that it was possible to impose positive as well as negative chirp to the fifth harmonic. This chirp was found to be different from that predicted by perturbation theory, equal to five times that of the fundamental chirp, by a negative amount, approximately equal to -300 μeV/fs ($= -4.6 \times 10^{26}$ s^{-2}). This chirp is rather small, implying that the accumulated phase by the electron wavepacket in the continuum is small, characteristic of a short excursion time. It could be due to different causes, from the single atom response to the propagation in the ionizing medium. More studies are necessary to pin down the origin of this small chirp inherent to the generation process.

These results led us to improve our experiment in order to be able to measure the chirp of higher order harmonics, with a better characterization of the pump and probe beams (see Fig. 5). Some results obtained with 50 fs IR pulses to generate harmonics and 50 fs probe pulses are presented in Figure 4, again with different conditions for the chirp of the fundamental IR pulse.

In contrast to the results obtained with the frequency-doubled radiation, the observed sidebands now include contributions from the harmonics directly below and above, since they can be created through absorption of one harmonic plus or minus one laser photon. If the chirp induced were very different for two consecutive harmonics, the sidebands would exhibit a complex variation in energy and time delay. The present results indicate that the frequency variation is rather small and similar for the different harmonics. There is, however, a systematic variation in the slope observed as a function of the harmonic order. The slope is clearly positive for the first sidebands of Figure 4 (top), decreases and becomes negative for the highest sidebands. A positive chirp added to the fundamental beam, by propagating it through 1 cm BK7 glass, (see Fig. 4 (bottom)) increases the chirp of the harmonics, especially for higher orders, in qualitative agreement with what can be expected.

Figure 5 summarizes these results more quantitatively. The term "sideband order" is used to denote the photoelectron peak corresponding to a net absorption of a certain number of infrared photons. The chirp is defined as the observed slope corrected by equation (1). It includes contributions from two harmonics (for "sideband order n", the $(n-1)$ and $(n+1)$th harmonic). In the same way, the extrapolated pulse duration reflects the contributions from two harmonics. The harmonics were found to exhibit only

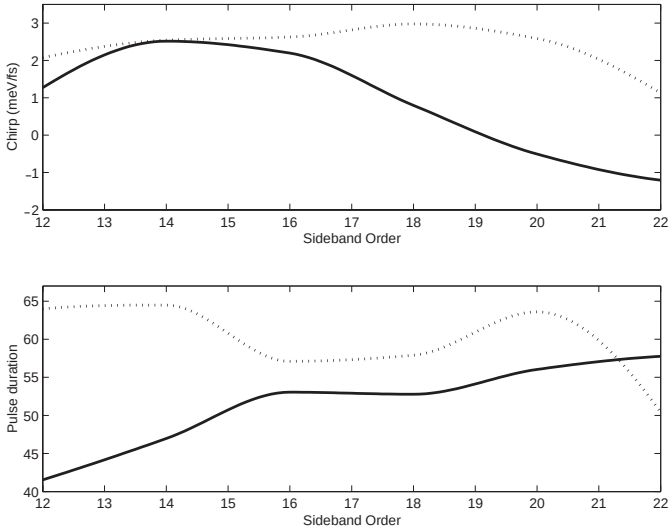

Fig. 5. Linear chirp (a) and pulse duration (b) of the harmonic pulses as a function of sideband order extracted from the data in Figure 4 for an unchirped (straight line) and chirped (dotted line) generating pulse.

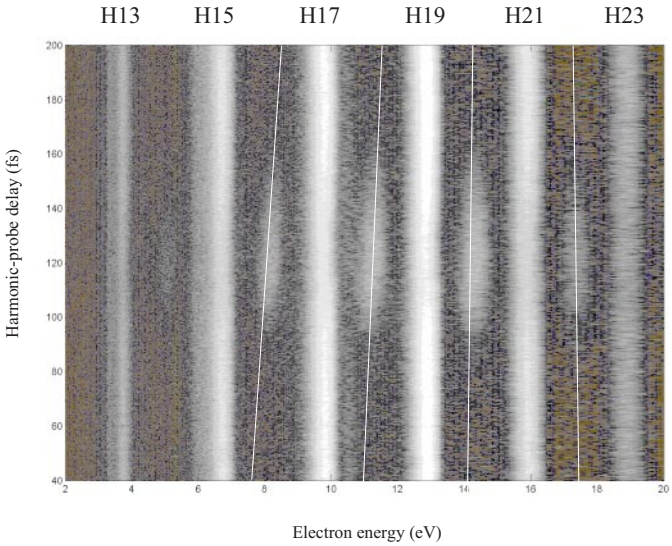

Fig. 6. Electron signal as a function of kinetic energy and time delay with a short probe pulse.

a small chirp, varying slowly with harmonic order. The chirp increased when 1 cm glass (BK7) was inserted in the beam before the harmonic generator, but not as much as was expected from the change in the fundamental.

A limiting factor in these experiments is the long duration of the probe pulse, as well as the 8 degree angle between pump and probe beams in the interaction region. We have recently improved our setup by setting pump and probe beams in an almost collinear geometry as well as by using shorter probe pulses. These pulses of duration sub-10 fs are obtained by using self-phase modulation in a hollow fiber followed by compression with chirped mirrors [18]. A first result is shown in Figure 6. The order-dependence of the chirp is clearly visible, as underlined by the white guidelines. The cross-correlation width of the sidebands is now much shorter than in the previous measurements, leading to pulse durations for the harmonics on the order of 20 fs. This setup has recently been used to investigate the temporal confinement of the harmonic radiation [19] using a generating pulse with a time-dependent ellipticity [20–22].

4 Conclusion

In summary, we have reported our progress in measuring pulse duration and frequency variation of high-order harmonics, using an energy-resolved cross-correlation method. Our next step will be to study in details the influence of the experimental conditions on the time-frequency behaviour of the harmonics, using well characterized generating and probe pulses as well as probe pulses of shorter duration than the harmonic pulses. This should lead not only to a better understanding of the harmonic generation process, but ultimately to precise control of the harmonic properties such as pulse length, spectral shape, and temporal coherence.

Support from the Göran Gustafsson Foundation for research in natural sciences and medicine, the Swedish Science Council, the Knut and Alice Wallenberg Foundation, and the European Community (ATTO network HPRN-CT-2000-00133), is gratefully acknowledged.

References

1. M. Lewenstein, P. Salières, A. L'Huillier, Phys. Rev. A **52**, 4747 (1995)
2. M.B. Gaarde, Opt. Expr. **8**, 529 (2001)
3. S.C. Rae, K. Burnett, J. Cooper, Phys. Rev. A **50**, 3438 (1994)
4. T.E. Glover, A.H. Chin, R.W. Schoenlein, Phys. Rev. A **63**, 023403-1 (2001)
5. J. Norin, J. Mauritsson, A. Johansson, M.K. Raarup, S. Buil, A. Persson, O. Dühr, M.B. Gaarde, K.J. Schafer, U. Keller, C.-G. Wahlström, A. L'Huillier, Phys. Rev. Lett. **88**, 193901 (2002)
6. S. Zamith, V. Blanchet, B. Girard, J. Norin, J. Mauritsson, A. L'Huillier, J. Andersson, S.L. Sorensen, I. Hjelte, O. Björneholm, D. Gauyacq, J. Chem. Phys. (in press, 2003)
7. A. L'Huillier, A. Johansson, J. Norin, J. Mauritsson, C.-G. Wahlström, Eur. Phys. J. D **26**, 91 (2003)
8. P.M. Paul, E.S. Toma, P. Breger, G. Mullot, F. Augé, Ph. Balcou, H.G. Muller, P. Agostini, Science **292**, 1689 (2001)
9. M. Hentschel, R. Klenberger, Ch. Spielmann, G.A. Reider, N. Milošević, T. Brabec, P. Corkum, U. Heinzmann, M. Drescher, F. Krausz, Nature **414**, 511 (2001)
10. M.B. Gaarde, K. Schafer, Phys. Rev. Lett. **89**, 213901 (2002)
11. A. Bouhal, P. Salières, P. Breger, P. Agostini, G. Hamoniaux, A. Mysyrowicz, A. Antonetti, R. Constantinescu, H.G. Muller, Phys. Rev. A **58**, 389 (1998)

12. T.E. Glover, R.W. Schoenlein, A.H. Chin, C.V. Shank, Phys. Rev Lett. **76**, 2468 (1996)
13. E.S. Toma, H.G. Muller, P.M. Paul, P. Breger, M. Cheret, P. Agostini, C. Le Blanc, G. Mullot, G. Cheriaux, Phys. Rev. A **62**, 061801 (2000)
14. M. Drescher, M. Hentschel, R. Kienberger, G. Tempea, C. Spielmann, G.A. Reider, P.B. Corkum, F. Krausz, Science **291**, 1923 (2001)
15. T. Sekikawa, T. Katsura, S. Miura, S. Watanabe, Phys. Rev. Lett. **88**, 193902 (2002)
16. C. Iaconis, I.A. Walmsley, Opt. Lett. **23**, 792 (1998)
17. This work has been done in collaboration with P. O'Keefe, M. Meyer, LURE, Orsay, France
18. M. Nisoli, S.D. Silvestri, O. Svelto, R. Szipocs, K. Frencz, C. Spielmann, S. Sartania, F. Krausz, Opt. Lett. **22**, 522 (1997)
19. This work has been done in collaboration with E. Constant, E. Mevel, O. Tcherbakoff, J. Plumridge, A. Zaïr, CELIA, University of Bordeaux, France
20. P.B. Corkum, N.H. Burnett, M.Y. Ivanov, Opt. Lett. **19**, 1870 (1994)
21. E. Constant, V.D. Taranukhin, A. Stolow, P.B. Corkum, Phys. Rev. A **56**, 3870 (1997)
22. C. Altucci, C. Delfin, L. Roos, M.B. Gaarde, I. Mercer, T. Starczewski, A. L'Huillier, C.-G. Wahlström, Phys. Rev. A **58**, 3934 (1998)